

Vacancy-mediated three-center four-electron bonds in GeTe-Sb₂Te₃ phase-change memory alloysAlexander V. Kolobov,^{1,2,*} Paul Fons,^{1,2} Junji Tominaga,¹ and Stanford R. Ovshinsky^{3,†}¹*Nanoelectronics Research Institute, National Institute of Advanced Industrial Science & Technology, Tsukuba Central 4, Higashi 1-1-1, Tsukuba, Ibaraki 305-8562, Japan*²*Spring-8, Japan Synchrotron Radiation Institute (JASRI), Kouto 1-1-1, Sayo-cho, Sayo-gun, Hyogo 679-5148, Japan*³*Ovshinsky Innovations LLC, 1050 East Square Lake Road, Bloomfield Hills, Michigan 48304, USA*

(Received 26 February 2013; revised manuscript received 8 April 2013; published 22 April 2013)

Although GeTe-Sb₂Te₃ (GST) alloys are widely used in data storage, many fundamental issues are still under debate. Here, we demonstrate that the presence of vacancies in the crystalline phase has far-reaching consequences, namely, a triad of twofold coordinated Te atoms with lone-pair electrons generated around the vacancy enables the formation of soft three-center four-electron bonds, whose properties provide an explanation for the unusual characteristics of GST, in particular, the increase in local disorder upon crystallization, the co-existence of a very fast switching rate with a large property contrast, the possibility of a solid-solid amorphization process that excludes conventional melting, and the drastic difference in crystallization behavior between GST and the ideal binary GeTe. Anisotropy of the three-center bonds may serve as an additional degree of freedom for information recording and provide a unified explanation for a variety of unique effects observed in lone-pair semiconductors.

DOI: [10.1103/PhysRevB.87.165206](https://doi.org/10.1103/PhysRevB.87.165206)

PACS number(s): 61.43.Dq, 63.20.dk, 61.05.cj

Nanosecond-order phase transitions in so-called phase-change materials are currently widely used in optical memories such as digital versatile disk random-access memory (DVD-RAM) and also in recently commercialized electronic nonvolatile phase-change random access memory devices (PC-RAM). The basic idea behind phase-change recording is to utilize the optical and/or electronic property contrast between the crystalline and amorphous states first suggested by S. R. Ovshinsky back in the 1960s.¹ Years of intensive research have singled out the quasibinary GeTe-Sb₂Te₃ (GST) alloys. This class of compounds exhibits atypically large differences in optical/electronic properties between the crystalline and amorphous phases, high thermal stability of both phases, a fast switching rate, and excellent scalability, making them ideal materials for storage applications.²⁻⁴ At the same time, there have been no reports of commercial use of binary GeTe, although it has similar switching parameters. As only a small subset of possible compounds displays the required attributes for practical applications; further investigation of the switching mechanism on the atomistic scale in these materials—and hence a precise knowledge of the structure—is needed to enable prescient development.

The most significant achievements along the route to an atomistic understanding should be recalled. First was the finding, obtained from x-ray (Bragg)-diffraction analysis, that thin amorphous films of quasibinary GeTe-Sb₂Te₃ compositions crystallize into a metastable cubic (rocksaltlike) structure at temperatures around 160 °C,⁵ and it is this cubic phase of GST that reversibly switches into the amorphous phase during the phase-change process. The anion sublattice in the rocksaltlike structure was found to be fully occupied by Te atoms, whereas the cation sites were populated with a composition-dependent random mixture of Ge and Sb atoms and vacancies. The latter were argued to be an intrinsic feature of the crystalline phase⁶⁻⁸ but very little further details were provided.

The structure was characterized in early works as having an unusually large isotropic thermal factor indicating a large degree of structural disorder.⁵ The coordination numbers

in the crystalline phase are usually described as $N_{\text{Ge}} = 6$, $N_{\text{Sb}} = 6$, and $N_{\text{Te}} = 4.8$;⁹ the lower Te coordination being due to the presence of nearby vacancies. In order for Ge (and Sb) atoms to be sixfold coordinated, the bonding in the crystalline state of GeTe and GST has been suggested to be resonant,^{10,11} with (on average) less than two electrons per bond. (A review of the nature of bonding in materials with electron-rich networks from a chemical viewpoint has been given in Ref. 12.) Resonance would ideally require six identical interatomic distances and a soft potential for the central atom.

Subsequent extended x-ray-absorption fine structure (EXAFS) studies demonstrated that the rocksalt structure of GST is distorted, i.e., there are subsets of three shorter and three longer bonds (3 + 3 coordination), similar to the rhombohedral GeTe, which is one of the endpoints. Even the shorter Ge-Te bonds (approximately 2.83 Å), in both GeTe and GST, were found to be significantly longer than the sum of the covalent radii of the participating atoms ($r_{\text{Ge}} = 1.22$ Å and $r_{\text{Te}} = 1.35$ Å, the total being 2.57 Å).⁶ Additionally, a strong bonding energy hierarchy was reported for the short and long bonds in the ideal GeTe structure,¹³ i.e., the resonance in this case can only be partial. It was also found that, counterintuitively, the mean-square relative displacement (MSRD) that characterizes disorder in the bond lengths was larger in the crystalline phase than in the corresponding amorphous phase,^{6,14} a highly unusual observation making phase-change alloys a unique class of materials where the degrees of the long-range order and short-range order anticorrelate, i.e., *the establishment of long-range order proceeds along with bond-length disordering of the structure on the atomic scale* (Fig. 1).

As regards the amorphous phase, EXAFS measurements found that amorphization of the crystalline phase resulted in the *shortening* of both Ge-Te and Sb-Te bonds to a value corresponding to the sum of the covalent radii, with a concomitant decrease in MSRD.⁶ These findings are inconsistent with a simple randomization of a covalently bonded solid such as Ge or GaAs where, due to the anharmonicity of the interatomic potential, bonds get longer and weaker,^{15,16} and suggest a

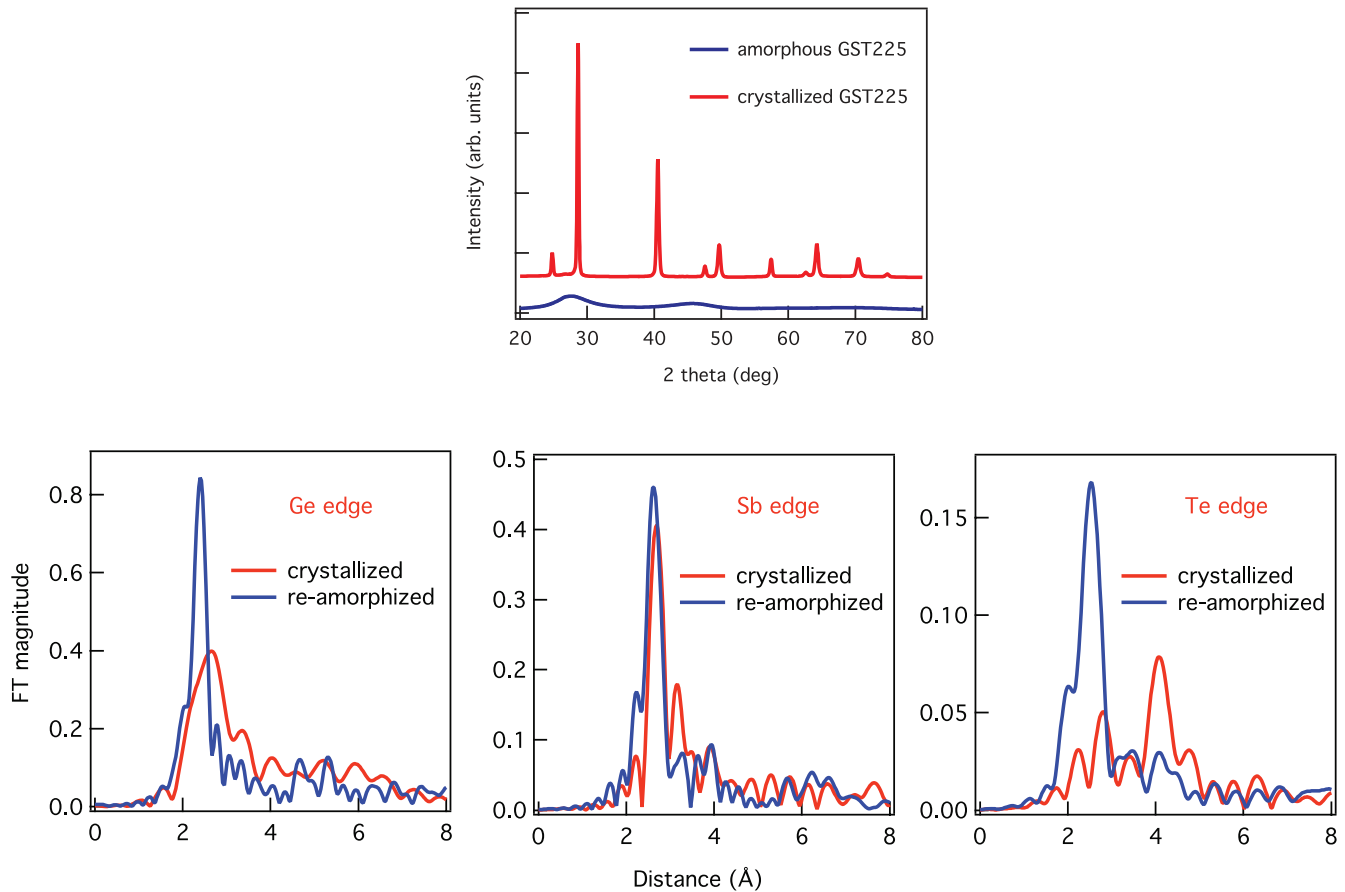


FIG. 1. (Color online) Comparison of x-ray-diffraction patterns (top) and Fourier transformed EXAFS spectra (bottom) for amorphous and crystallized phases of $\text{Ge}_2\text{Sb}_2\text{Te}_5$ demonstrates anticorrelation between the long-range and short-range order. Establishment of long-range order in the crystalline phase is evidenced by the appearance of sharp Bragg diffraction peaks. At the same time, the peaks in the Fourier transforms of EXAFS (reproduced after Ref. 6), especially at the Ge and Te K edges, become broader and have significantly lower intensity in the crystalline phase indicative of the increased disorder compared to the amorphous phase.

significant change in the local structure. Experimental and computational x-ray-absorption near-edge structure (XANES) studies suggested that the crystal-to-amorphous transition involved a switch of Ge atoms from octahedrally coordinated sites in the crystal to covalently bonded tetrahedrally and/or pyramidally (threefold) coordinated sites in the amorphous phase with associated local relaxation.^{6,17}

Density functional theory (DFT)-based *ab initio* molecular dynamics simulations performed on the melt-quenched amorphous phase of GST by different groups equally found the co-existence of tetrahedral Ge sites and fourfold coordinated sites with octahedral (i.e., approximately 90°) bonding angles. The latter had three shorter bonds and one longer bond and were described as defective octahedral sites, or pyramidal Ge sites.^{9,17–19} A small fraction of the defective octahedral sites had two longer bonds. The coordination numbers for Sb and Te atoms (using 3.2 \AA as a cutoff distance) were found to be close to 4 and 3, respectively,^{9,18} i.e., overcoordinated with respect to their usual valency. It should be noted that the results of DFT simulations are usually analyzed in terms of interatomic distances and bonding angles; the electron distribution is typically not analyzed, although it is the electron density distribution, rather than simply the atomic positions,

that determines the electronic properties of a material. It should also be noted here that while Ovshinsky has always stressed the importance of Te lone-pair electrons in determining the properties of phase-change alloys (see, e.g., Ref. 20] their exact role has remained veiled.

In this work, we demonstrate remarkable differences in bonding between binary GeTe and GST alloys that arise due to the presence of vacancies—and concomitantly Te atoms with lone-pair electrons—in the latter (but absent in the *ideal* binary GeTe). Through use of DFT simulations we demonstrate that Te lone-pair electrons serve to establish three-center four-electron Te-Ge-Te bonds characterized by a soft adiabatic potential. The Ge-Te bond softening in GST is experimentally confirmed through the analysis of temperature dependence of EXAFS. Finally, we demonstrate that the presence of the $3c-4e$ bonds has a drastic effect on the stability of the crystalline phase and may be the reason enabling commercial use of GST alloys (but not the binary GeTe material) in memory devices.

In order to characterize the interatomic bonding character, we have chosen to use the charge density difference (CDD) between the structure in question and isolated pseudoatoms. The usefulness of the CDD approach to investigate the bonding nature is demonstrated in Fig. 2 where covalently bonded Si,

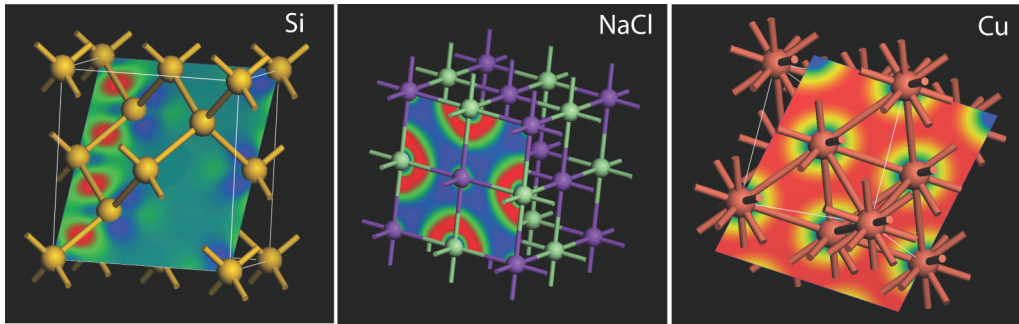


FIG. 2. (Color online) Comparison of CDD maps for Si (covalent bonds), NaCl (ionic bonds), and Cu (metallic bonds). The electron charge pileup (red spots midway between the Si atoms) is a signature of covalent bonding.

ionically bonded NaCl, and metallic Cu are compared. One can see that CDD has a simple physicochemical meaning: in particular, the electron charge pileup observed midway between the two (Si) atoms is a signature of covalent bonding. We use this feature to identify covalentlike bonding further in this work. Depending on the issue investigated, we have used both (i) two-dimensional CCD slices (maps) to represent the charge located on selected planes in two dimensions and/or (ii) CDD isosurfaces to determine areas of charge pileup in three dimensions where a 3D representation was required. A comparison of the two representations for the case example of silicon is shown in Fig. 3. It should be noted that the shown images are two different visualization methods to represent the same calculational result. One could arguably use alternative ways to analyze the bonding nature, such as the electron density distribution or electron localization function, but we believe that CDD—that by definition presents the difference in the charge distribution arising from bonding with neighbors in the structure under question—is more suitable. The electron density distribution analysis may involve unbonding electrons obscuring the picture and alternatives such as the electron localization function—as acknowledged by the CASTEP code developers—“may not be easy to interpret.”²¹ It may also be interesting to analyze the structures using maximally localized Wannier orbitals, which may provide additional information on the localization and role of individual orbitals.

Density functional calculations were carried out on a 64-atom cell using the plane-wave code CASTEP.^{22,23} Ultrasoft pseudopotentials were used for Ge, Sb, and Te atoms. The Ge

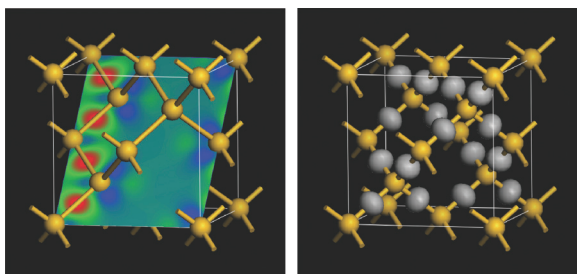


FIG. 3. (Color online) Two-dimensional (slice, left panel) and three-dimensional (isosurface, right panel) representations of charge density difference demonstrating the formation of covalent bonds, calculated for silicon using CASTEP code. Note that the two panels show the result of *the same* simulation.

and Te pseudopotential included the Ge $4s^2 4p^2$ and the Te $5s^2 5p^4$, as valence electrons, respectively. The exchange term was evaluated using the local density approximation from the numerical results of Ceperley and Alder²⁴ as parametrized by Perdew and Zunger.²⁵ The charge density was calculated with a plane-wave cutoff of 220 eV and a $2 \times 2 \times 2$ Monkhorst-Pack grid. For the relaxation processes the Broyden, Fletcher, Goldfarb, and Shannon algorithm²⁶ was used to relax the atomic coordinates at 0 K within a supercell of fixed volume; the volume was fixed to reflect the experimental determined density as conventionally done in the literature.

We start with a discussion of the unusual nature of Ge-Te bonding that is key in determining the structure of GeTe-based alloys. The local 3 (+3)fold bonding, with three covalentlike bonds and three weaker ones, as it exists in the rhombohedral GeTe is unusual for both Ge and Te atoms. Usually, Ge atoms are sp^3 hybridized and fourfold coordinated while chalcogens such as sulfur or selenium are twofold coordinated and possess lone-pair electrons, e.g., in $\text{GeS}(\text{e})_2$, where both elements satisfy Mott’s $8-N$ rule. Because the nonbonding lone-pair electrons of S(e) in these materials form the top of the valence band and consequently determine the materials properties, this class of materials is often called lone-pair semiconductors.²⁷

In the case of the rhombohedral GeTe, both Ge and Te atoms are 3 (+3)fold coordinated violating the $8-N$ formulation of the Mott rule. The Ge(3):Te(3) local bonding configuration becomes possible due to the rather weak localization of Te lone-pair electrons compared to S and/or Se and hence their ability to participate in bonding, where it becomes possible for both (unhybridized) Ge and Te atoms to form, in addition to two conventional covalent bonds with each element providing one electron per bond, an extra bond utilizing the Te lone-pair electrons and an empty p orbital of Ge, a so-called dative (or a donor-acceptor) bond.^{17,28,29}

To get more insight into the bonding nature in binary GeTe, Fig. 4 (upper panel) shows the structure of rhombohedral GeTe in the crystal coordinate system. Ge atoms are shown in blue and Te atoms are shown in orange. Because the shorter and longer bonds have a strong bonding energy hierarchy, as is demonstrated by the charge density difference (CDD) shown in the lower panel, the structure can be effectively viewed as covalently bonded Ge(3):Te(3) layers formed using the shorter bonds with significantly weaker forces (acting along the longer interatomic distances) holding the layers together, the situation being analogous to $\text{As}_2\text{S}(\text{e})_3$ where the covalently

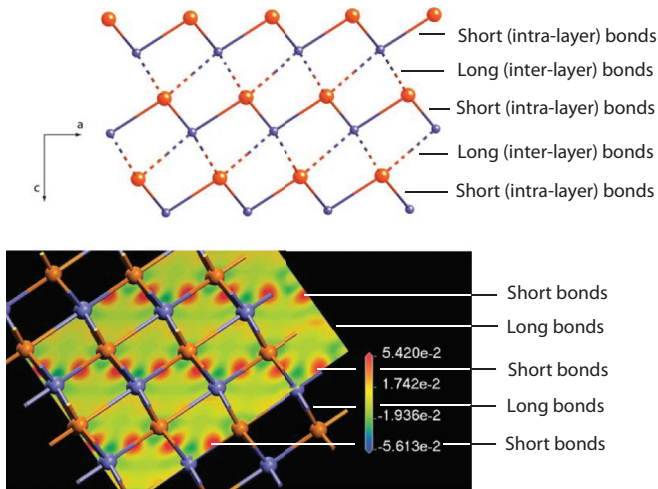


FIG. 4. (Color online) The structure of rhombohedral GeTe with shorter (solid lines) and longer (dashed lines) Ge-Te bonds (upper panel). Considering the strong bonding energy hierarchy between the shorter and longer bonds demonstrated by the CDD map (lower panel) obtained from DFT simulations, where the red shaded regions in the CDD map show the electron charge pileup along the shorter bonds that is indicative of covalent bonding, the structure can be effectively viewed as layered taking into account only the shorter Ge-Te bonds (a cutoff distance of 2.9 Å).

bonded layers interact through much weaker interlayer forces often referred to as van der Waals. The fact that *all* Te valence electrons in the ideal GeTe are consumed to form conventional covalent or dative bonds within layers means that GeTe—in stark contrast to $\text{As}_2\text{S}(e)_3$ and/or $\text{GeS}(e)_2$ —is not a lone-pair semiconductor. When a Ge vacancy is formed in a GeTe layer, because the origin of the electrons that form conventional covalent and dative bonds is different, despite the fact that *three* covalent Ge-Te bonds are broken, only *two* Te dangling bonds are formed; the third one reverts to a lone-pair orbital that cannot be used to form conventional covalent bonds.

How do vacancies, resulting from the incorporation (substitution) of Sb atoms, affect the structure of this type of material? An Sb atom has one unpaired valence electron on each of its three p orbitals and can thus form three conventional covalent bonds. On the other hand, Te atoms can form two conventional covalent bonds with Sb atoms; its lone-pair electrons cannot be used. As a result, removal of three Ge atoms from a GeTe layer generates six Te dangling bonds that are healed by two Sb atoms (shown in magenta in Fig. 5), i.e., only two Sb atoms are needed to replace three Ge atoms ensuring that all interatomic bonds are saturated, which determines the stability of the GeTe-Sb₂Te₃ tie line. This substitution generates a vacancy on a Ge site with a triad of Te atoms located next to the vacancy that are twofold coordinated and possess unused lone-pair electrons (Fig. 5). Because the Te atoms are low (twofold) coordinated, they can rather easily move in space (a soft mode) in the directions shown by the double-ended arrow. With 20% of Ge sites being vacant in a typical GST alloy Ge₂Sb₂Te₅, the concentration of lone pairs is on the order of 10^{21} cm^{-3} .

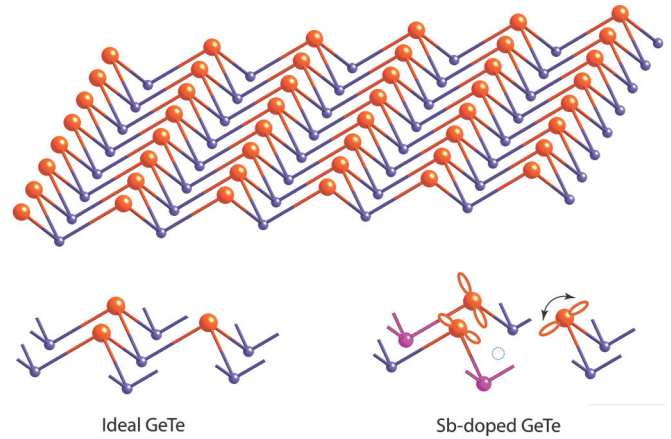


FIG. 5. (Color online) Top panel: a single buckled layer of the ideal GeTe. Lower panel (left) shows a smaller fragment of the layer including three Te atoms covalently (two conventional covalent bonds and one dative bond) bonded to Ge atoms. Both Ge and Te atoms are threefold coordinated and no lone-pair electrons exist. As a result of Sb doping (Sb atoms are shown in magenta) and different responses to the rupture of conventional covalent and dative bonds (see text), the Te atoms become twofold coordinated and possess p orbitals with lone-pair electrons, directed along the broken Ge-Te bonds (lower right-hand panel). The vacant Ge site is indicated by a dotted circle. Because of the low coordination numbers, the Te atoms can rather easily move in the directions indicated by the double-ended arrow.

How does the structural relaxation around vacancies proceed? In addition to the possibility that Te atoms move towards the vacancy, described previously in Refs. 30 and 31 and also confirmed by our simulations, an alternative scenario is also possible. Because the Te lone-pair orbitals are aligned with Ge-Te bonding orbitals in the neighboring layer, one can expect their overlap with the resulting formation of *3c-4e interlayer* Te-Ge-Te bonds. In this bonding configuration, two electrons from the pre-existing Ge-Te covalent bond within the upper layer and two lone-pair electrons from the Te atom located in the lower layer are shared between the three atoms. The central Ge atoms, whose single p orbital is used for bonding on both sides, effectively becomes fourfold coordinated (Fig. 6, upper panel). The covalent bonds, including three-center bonds, are shown by dual-color cylinders, where the color represents the origin of the bonding electrons. Thus, conventional covalent bonds, where each participating atom provides one electron per bond, shown as orange-blue and dative bonds, where both electrons are supplied by Te species, are orange-orange.

To verify this hypothesis, we have performed DFT simulations. The results (lower panel) show that there is indeed a charge pileup *on both sides* of the central Ge atoms with the identical “orange-orange” Ge-Te interatomic distances (2.97 Å), electron charge densities being very similar for both Ge-Te pairs, i.e., indeed, three-center Te-Ge-Te bonds, using one and the same p orbital of the central Ge atom, are formed.

It is important to note that the shown two-dimensional CDD maps only include charges located within the slice plane. For this reason, CDD for the two other (“orange-blue,” 2.86 Å) Ge-Te bonds, that are located out of the slice planes used, are not shown in the figure. (CDD on all four bonds for the same fragment are shown later in this paper when 3D isosurfaces

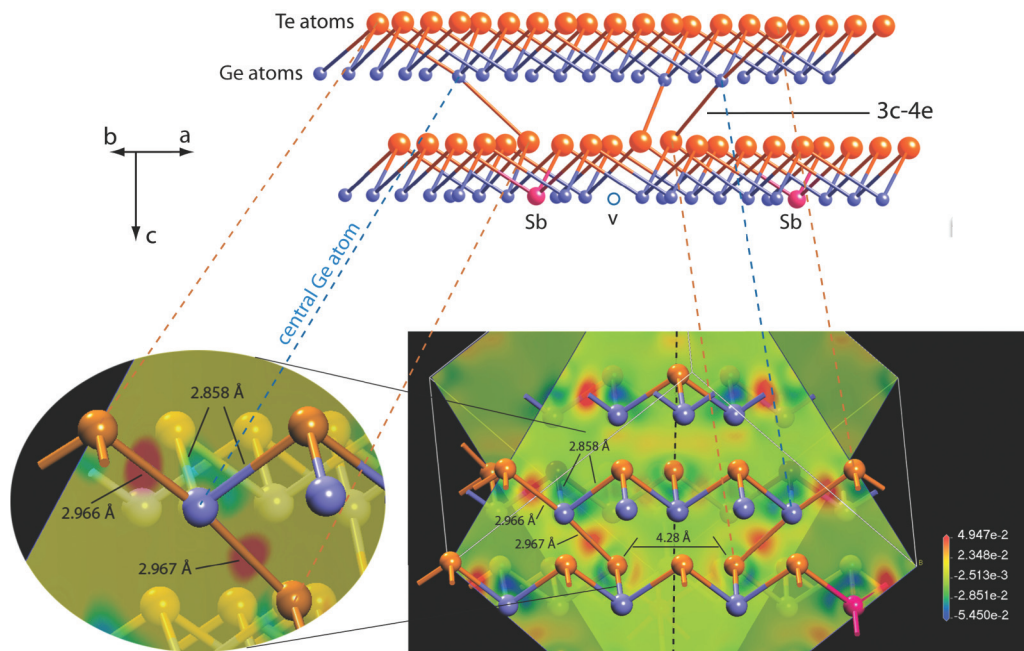


FIG. 6. (Color online) Schematic of the formation of three-center four-electron Te-Ge-Te bonds (upper panel) utilizing Te lone-pair electrons of the twofold coordinated Te atoms located around the Ge vacancy. Te atoms are shown in orange, Ge atoms in blue, Sb atoms in magenta, and the Ge-site vacancy is shown as an empty circle. The color of the covalent bonds represent the origin of the bonding electrons (see text for more detail). The lower panel shows the result of DFT simulation of the three-center Te-Ge-Te bond complexes. Two CDD slices—separated by a black dashed line—one for each of the two $3c-4e$ bonds, are shown on the right. The oval-shaped image on the left zooms into one of the three-center four-electron bonds. The CDD is projected onto a plane going through the atoms participating in the three-center bonds with the atoms in front of the slice being brighter in color than those behind the slice; the red spots of similar size and color midway between the Ge and Te atoms in the CDD map indicate covalent(like) interaction of similar strength on both sides of the central Ge atom along the Te-Ge-Te bond direction. Note that, because of the two-dimensional nature of the CDD maps, the charge distribution along the two other Ge-Te bonds (centered on the same Ge atoms) that are not contained within the slices used to visualize the CDD for the $3c-4e$ bonds is not shown.

rather than 2D slices are used to represent CDD, cf. Fig. 11, left-hand image.) Using the terminology proposed in Ref. 18 the shown fragment may be called a defective octahedral site. The consequences of its existence will be discussed later.

The fact that the *intralayer* Ge-Te bond length increases (from 2.83 Å to 2.97 Å) while the Ge-Te *interlayer* distance shrinks (from 3.17 to 2.97 Å) to exactly the same value clearly demonstrates that a new kind of bonding, a $3c-4e$ bond, is created in Ge-Sb-Te using the Te lone-pair electrons. It is interesting to note that the possibility of the formation of three-center bonds was suggested by Ovshinsky back in the 1970s,²⁸ but their existence has remained unconfirmed until now. The increased static local disorder in Ge-Sb-Te resulting from the atomic displacement around the three-center bonds due to the incorporation of Sb observed in our simulations (Fig. 7) is in agreement with the experimental results.³²

The creation of $3c-4e$ bonds has several important consequences. First, it leads to strengthening of interlayer interactions reducing the bonding energy hierarchy characteristic of the ideal binary rhombohedral GeTe and making the structure locally more “cubic” and less fragile than the ideal binary GeTe. Second, the similarity in the bond lengths and energies on the two sides of the central atom in the three-center bonds leads to a more conducive environment for resonance bonding in the structure with $3c-4e$ bonds, making quasibinary GeTe-Sb₂Te₃ different from the ideal GeTe case that is characterized by a strong bond energy hierarchy.

The *fundamental difference* between the Te-Ge-Te bonds in GST and bonding along the Te-Ge-Te direction in the ideal binary GeTe material is demonstrated in Fig. 8, which shows two CDD slices, one for each bonding configuration. While the

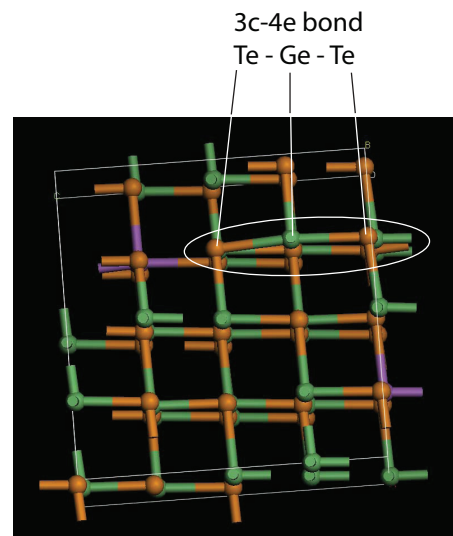


FIG. 7. (Color online) Local distortion around a $3c-4e$ bond in Sb-substituted GeTe resulting in an increased disorder of the crystalline phase.

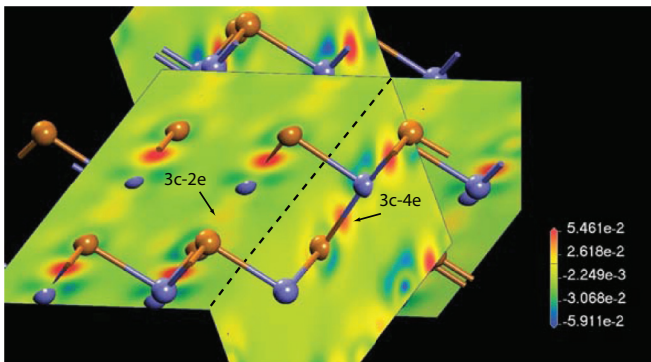


FIG. 8. (Color online) CDD maps comparing three-center two-electron ($3c-2e$) and three-center four-electron ($3c-4e$) bonds between the layers. While for the $3c-4e$ bond there is a charge pileup on both sides of the central Ge atom indicative of covalent(like) interactions, for the $3c-2e$ bond the charge is concentrated only along the shorter Ge-Te bond. The crystal orientation is the same as in Fig. 4.

longer Ge-Te bonds in GeTe are formed using the back lobes of the *same* p orbitals that form the shorter Ge-Te bonds, i.e., bonds along the Te-Ge-Te direction in GeTe are three-center *two-electron* ($3c-2e$) bonds. In GST, on the other hand, the Te-Ge-Te bonds are three-center *four-electron* bonds ($3c-4e$), the latter configurations being more stable and more symmetric, more polarizable, and serve to cross link the layers.

A major feature of the $3c-4e$ bonds is that they are at the same time strong and soft, i.e., highly polarizable,³³ and formally can be described in terms of an anharmonic interatomic potential.^{14,34} Experimental techniques that can be used to verify the existence of the $3c-4e$ bonds (e.g., vibrational spectroscopy) are very limited because the softer bonds in GST co-exist with heavier (Sb vs Ge) atoms. Possibly, the only direct experimental evidence for the formation of the much softer three-center bonds upon Sb substitution can be obtained from an Einstein analysis of the mean-square relative displacement (MSRD) obtained from EXAFS measurements. The uniqueness of this method is that it selectively probes the required type of bonds (Ge-Te in this case) independent of the structure of the material and other existing bonds. The extent to which the MSRD increases with temperature as well as its absolute value are determined by the bond stiffness, usually represented by the Einstein temperature Θ_E that is related to the MSRD σ through the following equation:

$$\sigma^2 = \frac{\hbar^2}{2\mu k_B \Theta_E} \coth\left(\frac{\Theta_E}{2T}\right) + \sigma_0^2. \quad (1)$$

Here, μ is the reduced mass, k_B is Boltzmann's constant, and σ_0 is static disorder. Figure 9 shows the experimental results for the Ge-Te bonds in binary GeTe and GST. From the slopes of the two curves one can readily see that Ge-Te bonds become significantly softer ($\Theta_E^{\text{Ge-Te}}$ changes from approximately 220 K to approximately 180 K, i.e., an almost 20% softening) upon inclusion of Sb atoms. This value agrees well with the bulk moduli B_0 of the two materials (49 GPa for GeTe vs approximately 40 GPa for GST).^{35,36} Although the change in the bulk modulus can also be associated with the larger concentration of vacancies in the latter, the

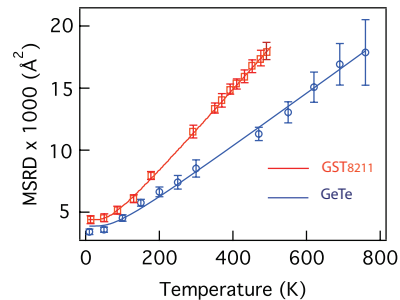


FIG. 9. (Color online) Temperature dependence of MSRD for Ge-Te bonds in binary GeTe and $\text{Ge}_8\text{Bb}_2\text{Te}_{11}$ demonstrating significantly softer Ge-Te bonds in the latter.

intermediate value of $B_0 = 44$ GPa in the hexagonal phase of GST that does not contain vacancies³⁷ suggests that the bonding nature plays an important role. For comparison, the Einstein temperature for the covalently bonded amorphous phases is significantly higher ($\Theta_E \approx 280$ K). The softness of the $3c-4e$ bonds may serve to accommodate interfacial stresses between the crystalline and amorphous phases generated in multiple switching cycles and account for why GST is a material of choice for memory applications while binary GeTe remains limited to academic pursuits. Along these lines, it was recently argued that failure of GeTe-based devices is caused by void formation associated with stresses, rather than with electric-field driven phase separation.³⁸

An increase in the concentration of Sb atoms increases the number of vacancies and, consequently, the number of twofold coordinated Te atoms with lone-pair electrons that can form three-center complexes. One can easily show that for the ideal $\text{Ge}_3\text{Sb}_2\text{Te}_6$ composition all Ge atoms and one-half of the Te atoms are involved in three-center complexes. What happens when the concentration of Sb atoms is increased further? One possibility is that three-center bonds along two and/or three orthogonal directions with the same central Ge atom can be formed. Alternatively, lone-pair electrons of the twofold coordinated Te atoms can interact with the Sb atoms in the neighboring layers creating Te-Sb-Te $3c-4e$ bonds. Detailed studies of this process require much larger simulation cells and are beyond the scope of this work.

The formation of the $3c-4e$ bonds that eliminate strong bond energy hierarchy between the *intra-* and *interlayer* Ge-Te distances has a drastic effect on the stability of the crystalline phase. In the ideal GeTe the long-range order is due to the weaker interaction between the back lobes ($3c-2e$ bonds), that is only possible when several, at least four, atoms within a -Ge-Te—Ge-Te- fragment, are aligned. Vibrations of the atomic system due to thermal or electronic excitation lead to temporal changes in interatomic distances and angles. Small-amplitude vibrations have no effect on the covalent bonds but the misalignment of atoms has a drastic effect on the back-lobe interaction. Once the atoms become misaligned, the weaker interlayer interaction is destroyed, i.e., the long-range order in the ideal GeTe material is intrinsically fragile. In an earlier publication¹³ we have demonstrated that excitation of specific vibrational modes in the system, namely such that misalign the covalently bonded fragments, leads to destruction of the weak back-lobe interaction resulting in a

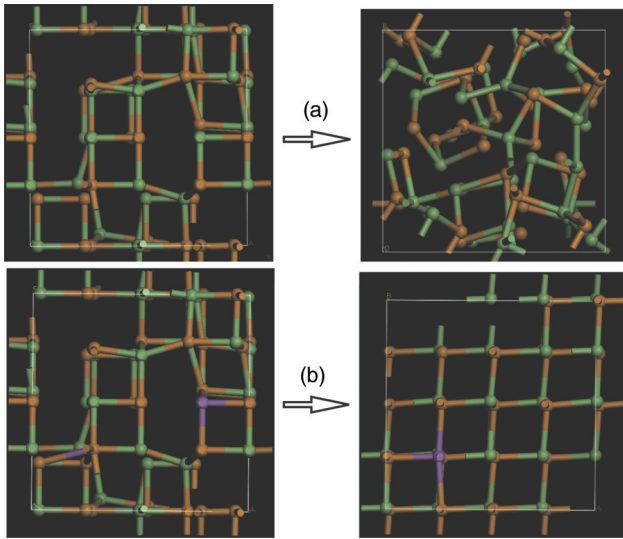


FIG. 10. (Color online) Relaxation of identically distorted crystalline structures for (a) the ideal GeTe material and (b) Sb-doped GeTe. Ge atoms are shown as green, Te atoms as orange, and Sb atoms as magenta balls, respectively. Bonds are shown (as dual-color) sticks between atoms located at distances smaller than 3 Å. See text for details.

loss of long-range order. The result is reproduced in Fig. 10 (top panel).

At the same time, in structures with $3c-4e$ bonds, the *interlayer* leg of the $3c-4e$ bond has the same length and strength as the *intralayer* leg which should make the long-range order more robust. To verify this hypothesis, we have performed DFT relaxation of a structure that was identical to the one used for the case of the ideal GeTe except that three Ge atoms were substituted by two Sb atoms (this ratio is determined by the stoichiometry of the quasibinary GST alloys) with the concomitant formation of one vacancy. One might naïvely expect that the presence of the vacancy would allow larger atomic displacements and should eventually result in easier amorphization. Counterintuitively, the distorted GST structure reverts to the crystalline phase (Fig. 10, lower panel), demonstrating that the three-center bonds, indeed, stabilize the crystalline phase.

An alternative interpretation of this result is that the formation of a $3c-4e$ bond acts as a nucleus for crystallization which provides an atomistic explanation for the fact that crystallization in GST is nucleation-dominant while in the ideal GeTe crystallization is growth dominant. The present finding is also in agreement with the experimental result that the crystallization becomes faster in GST alloys as the concentration of the Sb_2Te_3 component is increased.³⁹ Since the crystallization rate is the slowest process in PC-RAM, our finding provides a guideline for how to increase the crystallization rate.

The reported results also offer interesting insights into the phase-change mechanism. As described above, in the crystalline phase, Ge (and Sb) atoms in GST are involved in $4c-3e$ bonds with bonding angles close to 90° that can be alternatively described as defective octahedral sites. On the other hand, as consistently found by DFT simulations,

Ge (and also Sb) species in the amorphous phase also predominantly form defective octahedral sites^{17,18} with three shorter and nearly equal bonds and one (or two) longer bond. In other words, the defective octahedral sites are not formed upon amorphization as was tacitly suggested in the previous publications but pre-exist in the crystalline phase and one can view the phase-change (amorphization) process as consisting of the destruction of the three-center bonds with subsequent electron density redistribution leading to a corresponding decrease in polarizability. The transformation of a symmetrical three-center Te-Ge-Te bond with equal Ge-Te distances on both sides of the central Ge atom in the crystalline phase into an asymmetric structure with different Ge-Te distances in the amorphous phase is in perfect agreement with the Jahn-Teller theorem, from which it is known⁴⁰ that centrosymmetric structures that are locally unstable are only allowed in solids as a consequence of the long-range stabilizing forces that occur within a macroscopic periodic lattice. Destruction of the long-range order thus also implies the destabilization and destruction of the centrosymmetric three-center bond complexes. The reverse process upon the establishment of long-range order results in the formation of more symmetric structures. This process requires very small atomic displacements and hence can be extremely fast. The above description is rather simplified and aims at describing the core events responsible for the phase change contrast. The real process involves motion of the surrounding atoms and is more complex.

At the same time, the very small difference in the local *atomic* structure between the distorted octahedral sites in the crystalline and amorphous phases requiring very little atomic diffusion is accompanied by drastic changes in the nature of *electronic* interaction, which naturally accounts for the large electronic property difference between the two phases along with the very fast switching rates observed in GST alloys. This statement is illustrated in Fig. 11, where atomic configurations in the essentially identical “defective octahedral” Ge sites in

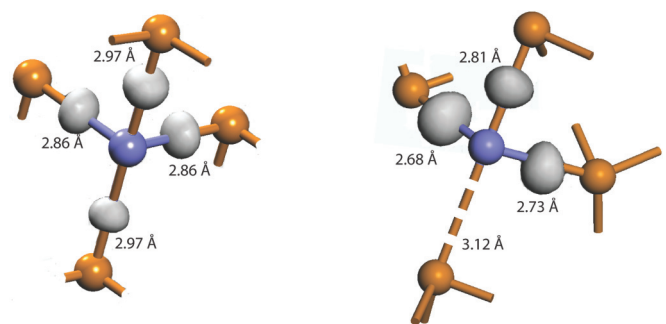


FIG. 11. (Color online) Fragments of “defective octahedral Ge sites” in the crystalline (left) and amorphous (right) phases with the corresponding CDD isosurfaces. Despite very similar *atomic* structures, indicating minute atomic motion, the character of interatomic interaction changes drastically as illustrated by the shown CDD isosurfaces (grey) obtained through DFT simulations. While in the crystalline phase the central Ge atom has covalentlike interactions with four Te neighbors, as evidenced by an electron charge pileup midway between the atoms, in the amorphous phase, it is covalently bonded to only three Te atoms. [The “amorphous” fragment is from a structure that we have studied in a previous work (Ref. 17).]

the crystalline and amorphous phases (fragments taken from the structures obtained through DFT simulations) and the corresponding CDD isosurfaces are compared: while in the crystalline phase the central Ge atom has covalentlike bonds with *four* Te neighbors, in the amorphous phase, the covalent interaction only exists with *three* neighbors along the shorter bonds. Realistic computer estimates of the switching time for both amorphization and crystallization processes require much larger simulation cells and are beyond the scope of this work.

Our results have important implications for practical use of the phase-change alloys. Thus they demonstrate that the softness of the three-center bonds may serve to accommodate stresses generated at crystal-amorphous interfaces due to the density difference between the two phases, permitting millions of cycles without noticeable property degradation, which may be the underlying reason for why $\text{Ge}_2\text{Sb}_2\text{Te}_5$ is one of the best commercially used phase-change alloys while the harder binary GeTe remains to be “a very promising material.” The importance of the density change upon crystallization has recently been shown to be an important factor for the formation of the glassy phase.⁴¹

Furthermore, the possibility of structural re-arrangement utilizing the softness of three-center bonds without conventional melting is of paramount importance from the application perspective in memory devices since melting is never good for device stability. In addition, melting is usually associated with entropic losses resulting in low energy efficiency. Some of the present authors demonstrated earlier that decreasing the entropic losses through use of layered structures such as interfacial phase-change materials (iPCMs) can increase the efficiency by more than 90%.⁴² This approach, based on switching that involves an athermal change in the bonding nature instead of the energy expensive melting process, has been adopted in the recently launched European project on universal memory development.⁴³

Finally, the obtained results may offer new possibilities for the design of phase-change memories. For example, by tuning the concentration and *spatial location* of Sb atoms one can control the three-center configurations. In particular, because the three-center bonds have their axes oriented along well defined crystalline directions, the electric field oriented in the same direction is more likely to couple with them and hence an anisotropic response can be expected, opening a new degree of freedom in information recording, for example by using linearly polarized light.⁴⁴ This may be of special interest in layered GeTe-Sb₂Te₃ structures prepared by means of digital-like growth procedures used in the fabrication of iPCM or by techniques such as molecular-beam epitaxy.^{45,46}

In summary, we have demonstrated that incorporation of Sb atoms into GeTe results in the generation of vacancies

surrounded by a triad of twofold coordinated Te atoms with lone-pair electrons. The presence of the latter in Ge-Sb-Te alloys (but not in the ideal binary GeTe) enables the formation of a variety of soft 3c-4e bonding configurations that account for the unusual crystallization behavior of GST where the long-range order is established at the expense of the local order. The softness of three-center bonds, co-existent with their strength, determines the properties of the crystalline phase and in particular determines the nucleation-dominant crystallization character in GST. It is also likely to be the reason for GST being a material of choice for commercial phase-change memory devices, as the soft 3c-4e bonds serve to accommodate interfacial stresses due to density difference between the crystalline and amorphous phases generated in multiple cycles suggesting the importance of such bonds for *practically usable* phase-change memory alloys.

We have further shown that destabilization of centrosymmetric 3c-4e bonds caused by the loss of long-range order, that results in the minute differences in the atomic structure between “defective octahedral” sites in the crystalline and amorphous phases, is accompanied by drastic changes in the character of interatomic bonding, being the key to the very fast switching speed combined with a large property contrast between the two phases. High polarizability of 3c-4e bonds is favorable for athermal switching paving the way to an increase in efficiency of phase-change memory devices. It is also proposed that by modifying the local structure through precise location and orientation of the three-center bonds, one can fine tune the properties of phase-change alloys, e.g., making use of the anisotropy of the 3c-4e bonds. Detailed studies of different 3c-4e configurations and their interaction in GST alloys, especially in those that contain larger concentrations of Sb₂Te₃, require the use of larger simulation cells and powerful computer facilities and remain to be done.

We believe that the high polarizability of the lone-pair *p* orbitals and the extreme softness of the three-center bonds reported in this work may also be key to the establishment of a unified theory of structure and the unique properties of chalcogenides, such as threshold switching, electric-field induced nucleation, electronic excitation-induced athermal melting, etc.

Note added in proof. Recently, we became aware of Ref. 47, where the possibility of the formation of interlayer Te-Ge bonds in GeTe was proposed to account for the low formation energy of Ge vacancies.

This work was partly supported by the LEAP project. The authors (A.K. and P.F.) acknowledge SPring-8 for provision of beam time for the EXAFS measurements.

*a.kolobov@aist.go.jp

†Deceased.

¹S. Ovshinsky, *Phys. Rev. Lett.* **21**, 1450 (1968).

²T. Ohta and S. R. Ovshinsky, *Photo-Induced Metastability in Amorphous Semiconductors* (Wiley-VCH, Weinheim 2003), pp. 310–326.

³M. Wuttig and N. Yamada, *Nat. Mater.* **6**, 824 (2007).

⁴A. V. Kolobov and J. Tominaga, *Chalcogenides: Metastability and Phase-Change Phenomena* (Springer, Berlin, 2012).

⁵N. Yamada and T. Matsunaga, *J. Appl. Phys.* **88**, 7020 (2000).

⁶A. Kolobov, P. Fons, A. Frenkel, A. Ankudinov, J. Tominaga, and T. Uruga, *Nat. Mater.* **3**, 703 (2004).

⁷T. Matsunaga, R. Kojima, N. Yamada, K. Kifune, Y. Kubota, Y. Tabata, and M. Takata, *Inorg. Chem.* **45**, 2235 (2006).

- ⁸M. Wuttig, D. Lüsebrink, D. Wamwangi, W. Welnic, M. Gillessen, and R. Dronskowski, *Nat. Mater.* **6**, 122 (2007).
- ⁹J. Akola and R. O. Jones, *Phys. Rev. B* **76**, 235201 (2007).
- ¹⁰G. Lucovsky and R. White, *Phys. Rev. B* **8**, 660 (1973).
- ¹¹K. Shportko, S. Kremers, M. Woda, D. Lencer, J. Robertson, and M. Wuttig, *Nat. Mater.* **7**, 653 (2008).
- ¹²G. A. Papoian and R. Hoffmann, *Angew. Chem. Int. Ed.* **39**, 2408 (2000).
- ¹³A. V. Kolobov, M. Krbal, P. Fons, J. Tominaga, and T. Uruga, *Nat. Chem.* **3**, 311 (2011).
- ¹⁴T. Matsunaga, N. Yamada, R. Kojima, S. Shamoto, M. Sato, H. Tanida, T. Uruga, S. Kohara, M. Takata, P. Zalden *et al.*, *Adv. Funct. Mater.* **21**, 2332 (2011).
- ¹⁵M. Ridgway, C. Glover, G. Foran, and K. Yu, *J. Appl. Phys.* **83**, 4610 (1998).
- ¹⁶M. Ridgway, G. Azevedo, C. Glover, K. Yu, and G. Foran, *Nucl. Instrum. Methods Phys. Res. B* **199**, 235 (2003).
- ¹⁷M. Krbal, A. V. Kolobov, P. Fons, J. Tominaga, S. R. Elliott, J. Hegedus, and T. Uruga, *Phys. Rev. B* **83**, 054203 (2011).
- ¹⁸S. Caravati, M. Bernasconi, T. Kühne, M. Krack, and M. Parrinello, *Appl. Phys. Lett.* **91**, 171906 (2007).
- ¹⁹J. Hegedüs and S. Elliott, *Nat. Mater.* **7**, 399 (2008).
- ²⁰*Disordered Materials: Science and Technology (Selected papers by Stanford R. Ovshinsky)*, edited by D. Adler, B. B. Schwartz, and M. Silver (Plenum, New York, 1991).
- ²¹CASTEP help page.
- ²²S. Clark, M. Segall, C. Pickard, P. Hasnip, M. Probert, K. Refson, and M. Payne, *Z. Kristallogr.* **220**, 567 (2005).
- ²³M. Segall, P. J. D. Lindan, M. Probert, C. Pickard, P. Hasnip, S. Clark, and M. Payne, *J. Phys.: Condens. Matter* **24**, 2717 (2002).
- ²⁴D. M. Ceperley and B. J. Alder, *Phys. Rev. Lett.* **45**, 566 (1980).
- ²⁵J. P. Perdew and A. Zunger, *Phys. Rev. B* **23**, 5048 (1981).
- ²⁶D. D. Johnson, *Phys. Rev. B* **38**, 12807 (1988).
- ²⁷M. Kastner, *Phys. Rev. Lett.* **28**, 355 (1972).
- ²⁸S. R. Ovshinsky and D. Adler, *Contemp. Phys.* **19**, 109 (1978).
- ²⁹M. Xu, Y. Q. Cheng, H. W. Sheng, and E. Ma, *Phys. Rev. Lett.* **103**, 195502 (2009).
- ³⁰C. Lang, S. A. Song, D. N. Manh, and D. J. H. Cockayne, *Phys. Rev. B* **76**, 054101 (2007).
- ³¹S. Caravati, M. Bernasconi, T. D. Kuehne, M. Krack, and M. Parrinello, *J. Phys.: Condens. Matter* **21**, 255501 (2009).
- ³²M. Krbal, A. V. Kolobov, P. Fons, R. E. Simpson, T. Matsunaga, J. Tominaga, and N. Yamada, *Phys. Rev. B* **84**, 104106 (2011).
- ³³S. Dembovskii and E. Chechetkina, *Glass Formation* (Nauka, Moscow, 1990).
- ³⁴V. G. Karpov, M. I. Klinger, and P. N. Ignatiev, *Solid State Commun.* **44**, 333 (1982).
- ³⁵A. Onodera, I. Sakamoto, Y. Fujii, N. Mōri, and S. Sugai, *Phys. Rev. B* **56**, 7935 (1997).
- ³⁶A. V. Kolobov, J. Haines, A. Pradel, M. Ribes, P. Fons, J. Tominaga, Y. Katayama, T. Hammouda, and T. Uruga, *Phys. Rev. Lett.* **97**, 035701 (2006).
- ³⁷M. Krbal, A. V. Kolobov, J. Haines, P. Fons, C. Levelut, R. Le Parc, M. Hanfland, J. Tominaga, A. Pradel, and M. Ribes, *Phys. Rev. Lett.* **103**, 115502 (2009).
- ³⁸A. Bastard, J. C. Bastien, B. Hyot, S. Lhostis, F. Mompiau, C. Bonafos, G. Servanton, C. Borowiak, F. Lorut, A. Bicaiss-Lepinay, N. Toffoli *et al.*, *Appl. Phys. Lett.* **99**, 243103 (2011).
- ³⁹N. Yamada, E. Ohno, N. Akahira, K. Nishiuchi, K. Nagata, and M. Takao, *Jpn. J. Appl. Phys.* **26-4**, 61 (1987).
- ⁴⁰I. B. Bersuker, *The Jahn-Teller Effect* (IFI/Plenum, New York, 1983).
- ⁴¹Y. Li, Q. Guo, J. A. Kalb, and C. V. Thompson, *Science* **322**, 1816 (2008).
- ⁴²R. E. Simpson, P. Fons, A. V. Kolobov, T. Fukaya, M. Krbal, T. Yagi, and J. Tominaga, *Nat. Nanotechnol.* **6**, 501 (2011).
- ⁴³http://cordis.europa.eu/search/index.cfm?fuseaction=proj.document&PJ_RC�=13130107.
- ⁴⁴K. Makino, J. Tominaga, A. V. Kolobov, P. Fons, and M. Hase, *Appl. Phys. Lett.* **101**, 232101 (2012).
- ⁴⁵W. Braun, R. Shayduk, T. Flissikowski, M. Ramsteiner, H. T. Grahn, H. Riechert, P. Fons, and A. Kolobov, *Appl. Phys. Lett.* **94**, 041902 (2009).
- ⁴⁶P. Rodenbach, R. Calarco, K. Perumal, F. Katmis, M. Hanke, A. Proessdorf, W. Braun, A. Giussani, A. Trampert, H. Riechert *et al.*, *Phys. Status Solidi (RRL)* **6**, 415 (2012).
- ⁴⁷B. Huang and J. Robertson, *J. Non-Cryst. Solids* **358**, 2393 (2012).